# Interfacial Fracture in Compliant Substrate Film Systems

M. S. Kennedy[1], M. J. Cordill[2], J. Yeager[3], I. Rook[1], D. P. Adams[4], E. D. Reedy, Jr.[4], J. A. Emerson[4], D. F. Bahr[3], N. R. Moody[5]

*[1]Clemson University, Clemson, SC, USA, [2]Erich Schmid Institute, Leoben, Austria, [3]Washington State University, Pullman, WA, USA, [4]Sandia National Laboratories, Albuquerque, NM, USA, [5]Sandia National Laboratories, Livermore, CA, USA*

## Abstract

Reliability of thin hard films on compliant substrates is a key factor governing the use of emerging flexible substrate devices where compressive stresses can lead to delamination and buckling. Previous modeling of buckle-driven delamination in hard film-compliant substrate systems has shown the importance of elastic mismatch on fracture morphologies and measured fracture energies. This study highlights the contributions of plastic deformation during fracture between rigid films and relatively compliant substrates. Depositing 100 nm and 200 nm thick W films onto silicon and PMMA substrates that spanned two orders of magnitude in stiffness triggered Euler and telephone cord buckles that varied markedly in morphology with substrate compliance. For films on PMMA, buckling was accompanied by significant substrate deformation and yielding. In this paper we show how substrate compliance, deformation, and yielding affect buckle formation, susceptibility to interfacial fracture, and fracture energies in hard elastic films on compliant substrates.

## 1. Introduction

Development of flexible thin film systems for biomedical, homeland security and environmental sensing applications has increased dramatically in the last five years [1,2]. These systems typically combine traditional semiconductor technology with new flexible substrates, allowing for both the high electron mobility of semiconductors and the flexibility of polymers. The devices have the ability to be easily integrated into components and show promise for advanced design concepts, ranging from innovative microelectronics to MEMS and NEMS devices. Deformation and fracture are critical factors controlling the performance and reliability of these systems, and in all cases depend on film adhesion. Adhesion of polymer-metal interfaces has been studied using tape [3], pull off [4], and peel tests [5]. More recent techniques for measuring adhesion include spontaneous blisters [6,7] and stressed overlayers [16]. In both the spontaneous blister and stressed overlayer methods, the thin films are subjected to appreciable residual stresses that trigger delamination and fracture.

There is a large body of elastic solutions describing delamination and buckling of films from rigid substrates, linking buckle morphology to interfacial fracture energy [8,9,10,11].These models, however, cannot be directly applied to films on compliant substrates. Recent models by Yu and Hutchinson [12] and Parry and

co-workers [13], have modified these solutions by incorporating the ratio between film and substrate moduli. Work by Coterell et al. [14] and Yu and co-workers [12] show that substrate compliance has a marked effect on fracture energies and phase angles of loading. Increasing substrate compliance increases the mode *I* contribution thereby promoting failure. Yu and Hutchinson [12] examined these systems using two approaches, which included both strain energy release rate and the total energy of the system as a function of the film stress, $\sigma_f$, modulus, $E_f$, and Poisson's ratio, $\nu_f$. In this study, the models of Yu and Hutchinson [12] and Parry and co-workers [13] are used to analyze the role of substrate compliance on interfacial fracture of 100 nm and 200 nm thick W films deposited onto PMMA with and without a 10 nm $Al_2O_3$ interlayer.

## 2. Experimental

To determine the mechanical response of W films on compliant substrates, 100 nm thick W films were deposited onto sapphire ($Al_2O_3$), fused quartz, silicon and PMMA. A second set PMMA substrates were also prepared with a 10 nm $Al_2O_3$ interlayer. Thin film and substrate properties were measured using a MTS Nano Instruments Nano Indenter® XP and a Nano Indenter® DCM with Berkovich diamond indenters. For tests on the XP, a frequency of 45 Hz, amplitude of 2 nm and maximum depth of 1000 nm was used. With DCM testing, a frequency of 75 Hz, amplitude of 1 nm and maximum depth of 500 nm was used. A second set of PMMA substrate samples was created by depositing 200 nm of W onto PMMA, with and without a 10 nm $Al_2O_3$ interlayer. Residual stress in the W films was monitored by wafer curvature measurements on a silicon monitor. Once delamination was observed, a Digital Instruments multimode Atomic Force Microscope (AFM) was used to characterize blister heights and widths using both tapping and contact modes. The films were then removed and the substrates were imaged with tapping mode to characterize deformation on the substrate surfaces.

## 3. Results and Discussion

### 3.1 Properties

Nanoindentation showed a strong effect of substrate compliance on measured properties. Near surface modulus (Fig. 1) and hardness (Fig. 2) values for hard substrate systems (sapphire and silicon) matched bulk properties for tungsten (E=410 GPa, H=12-15 GPa). However, the properties measured in more compliant substrate systems (fused quartz and PMMA) were markedly lower than those measured in rigid substrate systems (silicon and sapphire) due to substrate deformation. True properties of the W films are the same for all these systems. The low values measured in the compliant substrate systems are caused in part by determining the contact area from indenter displacement rather than true contact area from direct observation. Modulus and hardness values for all substrates with an $Al_2O_3$ interlayer exhibited the same behavior as systems without an interlayer, but values were slightly lower. Earlier work by Pharr and co-workers [15]

showed that sputter deposited aluminum oxide formed an amorphous film with a modulus near 150 GPa and hardness between 5-6 GPa. These values are lower than W and significantly lower than sapphire or alumina.

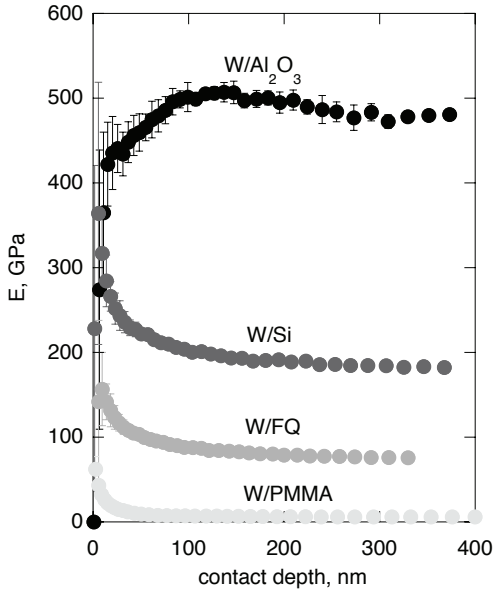


Figure 1: The near surface modulus values for 100nm W on sapphire and silicon matched bulk properties for tungsten, however, near surface modulus values for 100nm W on more compliant substrates were lower due to substrate deformation.

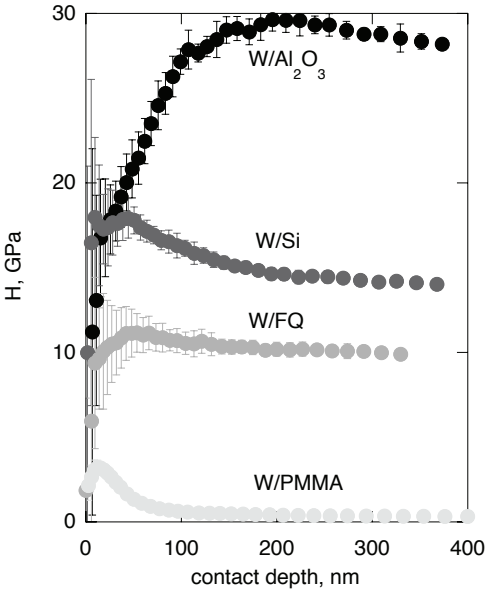


Figure 2: Hardness values for 100nm W films on sapphire, silicon, fused quartz and PMMA. The harder substrates allow for the approximation of hardness values close to the bulk properties of tungsten (H=12-15 GPa).

### 3.2 Delamination and Buckling

Buckles formed spontaneously following film deposition. On films with an $Al_2O_3$ interlayer, telephone cord buckles formed a widely spaced pattern of uniform width buckles. (Fig. 3a) On films without the $Al_2O_3$ interlayer, an extensive network of small telephone cord buckles formed following deposition, interspersed with regions of larger telephone cord buckles similar in size to those on the substrate with an interlayer. (Fig. 3b)

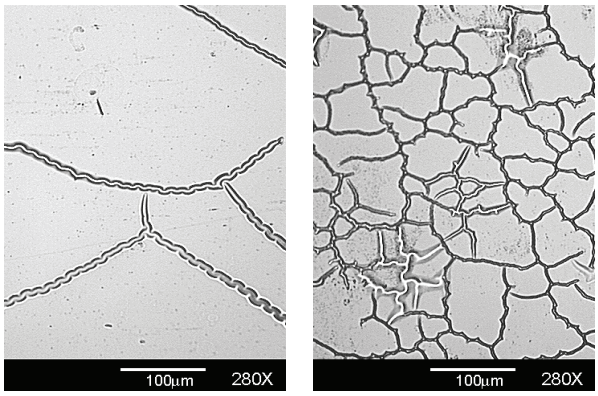


(a) (b)

Figure 3: Telephone cord blisters in tungsten on PMMA (a) with a 10 nm aluminum oxide interlayer and (b) without an interlayer.

### 3.3 Fracture Energies

The critical buckling stresses for the W/PMMA and W/$Al_2O_3$/PMMA systems were found using the rigid substrate-elastic film solutions of Hutchinson and Suo [16]. The residual stress, $\sigma_r$, of the W films, and the blister heights and widths measured with AFM, were used to calculate the energy release rate for plane strain ($\varepsilon_{zz}$=0) buckles, assuming a rigid elastic case. (Table 1) Wafer curvature showed the residual stress in these films was -1.7 GPa. The energy release rate, $\Gamma$, and phase angle of loading, $\psi$, were then determined from Yu and Hutchinson's solutions for normalized strain energy release using a stress intensity approach for $\alpha$=0.99 and $\sigma_r/\overline{E_f}$ equal to 0.01%, 0.1%, and 1%., where $\alpha$ is the elastic mismatch coefficient and $\overline{E_f} = E_f/(1-\nu^2)$ [12]. For the W on PMMA systems, $\sigma_r/\overline{E_f}$ is near 0.4%. The corresponding energy release rates for blisters in our systems were found by interpolating the Yu and Hutchinson $\sigma_r/\overline{E_f}$ solutions between 0.1% and 1%. The mode I release rates, $\Gamma_I$, were determined using the empirical relationships between mixed mode and mode I energies given by Hutchinson and Suo. [16]. The fracture energies determined using these solutions more than doubled from rigid elastic values for large buckles in the W/PMMA and W/$Al_2O_3$/PMMA systems and increased almost 8-fold for small buckles in the W/PMMA system. There was also a dramatic change in the phase angle of loading from pure shear in the W/Si system to predominantly mode I loading in the W/PMMA system with small buckles.

| Systems | Rigid Elastic | | | Yu & Hutchinson | | |
|---|---|---|---|---|---|---|
| | $\Gamma(\psi)$ J/m$^2$ | $\psi$ deg | $\Gamma_I$ J/m$^2$ | $\Gamma(\psi)$ J/m$^2$ | $\psi$ deg | $\Gamma_I$ J/m$^2$ |
| 200nm W/ $SiO_2$/ Si | 0.7 | -90 | 0.2 | 0.7 | -90 | 0.2 |
| 100nm W/ $Al_2O_3$/ PMMA | 0.4 | -63 | 0.2 | 0.9 | -63 | 0.5 |
| 100nm W/ PMMA | | | | | | |
| Large | 0.4 | -63 | 0.2 | 0.9 | -63 | 0.5 |
| Small | 0.4 | -33 | 0.3 | 2.7 | -33 | 1.9 |
| 200nm W/ $Al_2O_3$/ PMMA | 0.7 | -65 | 0.4 | 1.6 | -65 | 0.8 |
| 200nm W/ PMMA | 0.8 | -50 | 0.5 | 2.9 | -50 | 3.6 |

Table 1: Fracture energies of the systems are calculated using rigid elastic analysis and those presented by Yu and Hutchinson [12].

### 3.4 Fracture Processes

River markings formed on PMMA substrate surfaces when the films spalled and highlight the extent of the plastic zones that formed ahead of the crack tip at the edge of the buckles. (Fig. 4 and Fig. 5) They result from an increase in interfacial toughness between W and PMMA where crack tip plastic zones have formed in the substrate such that when the W film spalls, these regions deformed more extensively than surrounding regions. This is not observed in rigid substrate systems and strongly suggests that localized substrate yielding and localized plasticity influences behavior in these systems.

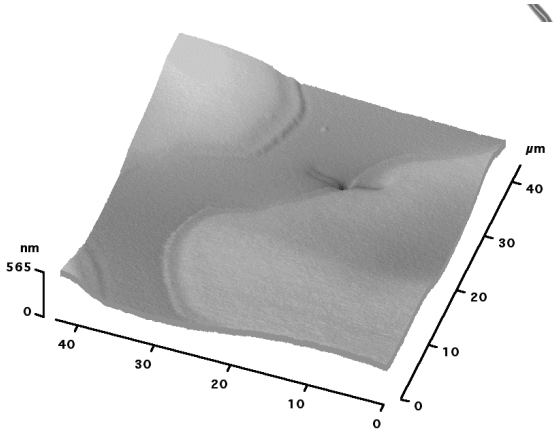


Figure 4: By lifting off the 200 nm W films after the formation of telephone cord blisters on the PMMA, river marks were seen to run along the same path as the blister. This indicated that there was severe plastic deformation under the film.

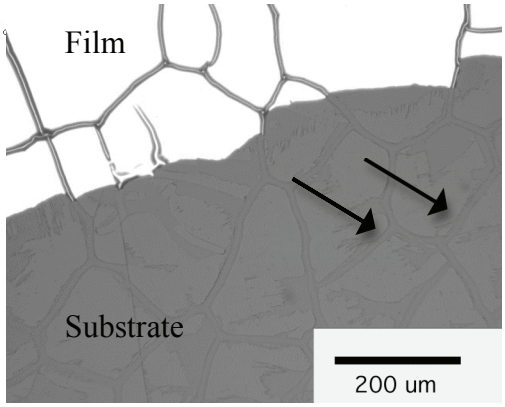


Figure 5: Scanning the substrate with tapping mode AFM, the formation of boundary markers were evident in the 200 nm W/ PMMA system. Arrows indicate the buckle footprints.

### 3.5 Buckle morphology

Parry et al. [13] showed that substrate compliance markedly alters the relationship between buckle deflection and stress using non-linear finite element simulations. They found that compliance could reduce the effective critical stress by up to fourty percent and increase deflections up to two-times that for a rigid substrate, depending on elastic mismatch. Parry and co-workers suggest that the effects can be addressed by using two correction factors such that the expression relating deflection to film stress becomes,

$$\frac{\delta}{h} = \gamma_\delta \sqrt{\frac{4}{3}\left(\frac{\sigma_r}{\gamma_\sigma \sigma_c} - 1\right)} \qquad (1)$$

where $\sigma_r$ is the residual stress in the film and $\sigma_c$ is the critical buckling stress. The correction factor for the critical stress, $\gamma_\sigma$, and the correction factor for the deflection, $\gamma_\delta$ , vary with $\alpha$ and are given by Parry et al. [13]. Using the rigid elastic solution for the W blisters observed on Si predicts a residual stress near -3.0 GPa. Correcting for substrate compliance gives a value of -2.0 GPa, when $\alpha$=0.5 for W/Si. It gives a value of -1.7 GPa for $\alpha$=0.7 W/$SiO_2$/Si. However, the height-to-width ratios were greater than elastic theory predicts for a -1.7 GPa residual stress as shown in Figure 6. Superimposing the non–dimensional buckle height data, $\delta/h$, from this study onto curves of $\delta/h$ vs. $\sigma_r/\sigma_c$ from Parry et al. [13], shows good agreement for large blister data. The smaller blisters found in the W/PMMA system exhibit markedly different behavior even when the effect of compliance is included in the analysis. AFM imaging clearly shows that the regions of deformation along small buckle walls are much larger and more intense than those along large blister walls. This deformation alters buckle morphology beyond the effects indicated by compliant substrate models. As a consequence, interfacial fracture energies calculated using elastic buckle theory even when the effect of compliance is included may not accurately describe the energy required for telephone cord blister formation.

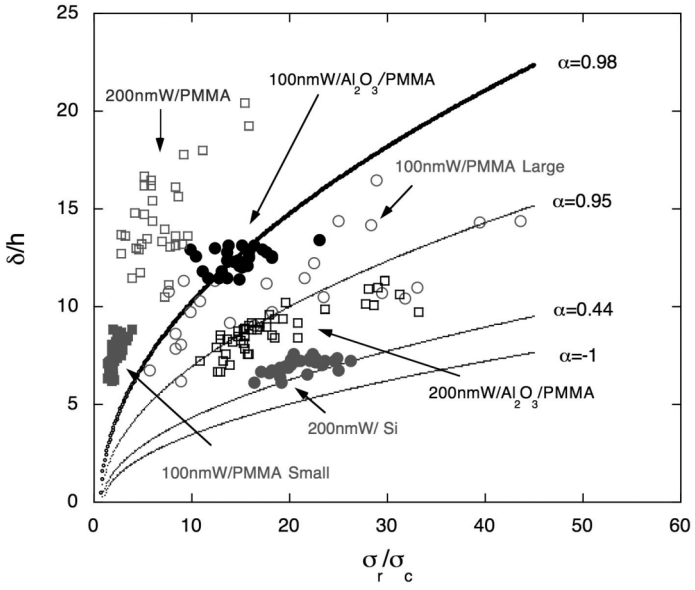


Figure 6: Superimposing the non–dimensional buckle height data, $\delta/h$, from this study onto curves of $\delta/h$ vs. $\sigma_r/\sigma_c$ from the work of Parry et al. [13] indicate that competing mechanisms not taken into account are influencing the fracture.

## 4. Conclusions

In this study, highly compressed tungsten films were sputter deposited onto silicon and PMMA substrates spanning two orders of magnitude in compliance with and without a 10 nm thick aluminum oxide interlayer. The films were sputter deposited to thicknesses of 100 nm and 200 nm with residual compressive stresses of 1.7 GPa. The interlayer was used to fix adhesion. Following deposition, buckles formed spontaneously on the PMMA substrates. There was a strong susceptibility to buckling in W/PMMA systems. An even greater effect of substrate compliance was observed on buckle morphology, where buckle heights increased markedly with substrate compliance. Substrate surface imaging revealed extensive deformation occurred along delaminations not observed in rigid substrate systems. The regions of deformation along small buckle walls are much larger and more intense than those along large blister walls. This highly localized deformation altered buckle morphology and fracture energies beyond the effects predicted by existing delamination or cracking models.

## Acknowledgements

The authors thank Kim Archuleta and Eric Jones of Sandia National Laboratories, Albuquerque, NM for film preparation. This work is supported by Sandia National Laboratories, a multiprogram laboratory operated by Sandia Corporation, a Lockheed Martin Company for the United States Department of Energy's National Nuclear Security Administration under contract DE-AC04-94AL85000.

---

## References

[1] K. Bock, Polytronics-electronics and systems on flexible substrates, IEEE VLSI-TSA 4 (53) (2005) 53-56.
[2] K. Jain, M. Klosner, M. Zemel, S. Raghunandan, Flexible electronics and displays: high-resolution, roll-to-roll, projection lithography and photoablation processing technologies for high-throughput production, *Proc IEEE* 93 (8) (2005) 1500-1510.
[3] P. Wu, T. Lu, Metal/polymer adhesion enhancement by reactive ion assisted interface bonding and mixing, Appl Phys Let 71 (1997) 2710-2712.
[4] W. Li, R. Charters, B. Luther-Davies, L. Mar, Applied Surface Science 2004, 233, 227.
[5] J. Yu, J. Song, I. Park, Analyses of the Practical Adhesion Strengths of the Metal/Polymer Interfaces in Electronic Packaging, Journal of Electronic Materials 2002, 31, 1347.
[6] M. George, C. Coupeau, J. Colin, F. Cleymand, J. Grilhe. Delamination of metal thin films on polymer substrates: from straight-sided blisters to varicose structures, Philosophical Magazine A, 2002, 82, 633.

[7] M. George, C. Coupeau, J. Colin, J. Grilhe, Mechanical behaviour of metallic thin films on polymeric substrates and the effect of ion beam assistance on crack propagation, Acta Materialia 2005, 53, 411.
[8] C. Brabec, J. Hauch, P. Schilinsky, C. Waldauf, Production aspects of organic photovoltaics and their impact on the commercialization of devices, MRS Bul 30 (1) (2005) 50-52.
[9] M. Thouless, J. Hutchinson, E. Liniger, Plane-strain, buckling-driven delamination of thin films: model experiments and mode-II fracture, Acta Met 40 (10) (1992) 2639-2649.
[10] T. Ye, Z. Suo, A. Evans, Thin film cracking and the roles of substrate and interface, Int Jour Sol Struct 29 (21) (1992) 2639-2648.
[11] H. Mei, R. Huang, J. Chung, C. Stafford, H.-H. Yu, Buckling modes of elastic thin films on elastic substrates, Appl Phys Let 90 (15) (2007) 151902.
[12] H.-H. Yu, J. Hutchinson, Influence of substrate compliance on buckling delamination of thin films, Inter Jour Fract 113 (2002) 39-55.
[13] G. Parry, J. Colin, C. Coupeau, F. Foucher, A. Cimetiere, J. Grilhe, Effect of substrate compliance on the global unilateral post-buckling of coatings: AFM observations and finite element calculations, Acta Mater 53 (2005) 441-447.
[14] B. Cotterell, Z. Chen, Buckling and cracking of thin film on compliant substrates under compression, Inter Jour Fract. 104 (2000) 169-179.
[15] T. Chou, T. Nieh, S. McAdams, G. Pharr, Microstructures and mechanical properties of thin films of aluminum oxide, Scripta Met 25 (10) 1991 2203-2208.
[16] J. Hutchinson, Z. Suo, Mixed-mode cracking in layered materials, Advances in Applied Mechanics, 29 (1992) 29-63.